Harmonic Compensation in Standalone Distributed Generation System

Mohit[1] and Sukhbir Singh

M.Tech Scholar, Department of Electrical Engineering[1]

Assistant Professor, Department of Electrical Engineering[2]

School of Engineering & Technology, Soldha, Bahadurgarh, Haryana, India

Abstract: *This dissertation deals with a dual second-order generalized integrator based frequency locked loop (DSOGI-FLL) control approach for a standalone distributed generation (DG) system under unbalanced nonlinear load condition and varying wind speed. The DG system consists of wind driven SEIG, interfacing inductors, voltage source convertor (VSC), battery storage system (BSS) and nonlinear load. The DSOGI-FLL algorithm with enhanced filtering capability, employed for both voltages and currents, helps to attenuate the harmonics, and estimates the sequence components. This algorithm elicits the fundamental component of highly nonlinear load current required for calculating the reference magnitude of the load currents. The proposed control with VSC provides multi-functions voltage/frequency regulation of SEIG, active/reactive power support, harmonics elimination, load balancing and improve the overall power quality of the DG system. The battery storage system (BSS) is connected at dc link of the VSC to provide power support during dynamic conditions. This system is simulated in MATLAB/ Simulink environment and results are analyzed under dynamic conditions. The simulation results are observed in accordance with the standard of the IEEE-519.*

Keywords: Battery storage system, Distributed generation system, frequency locked loop

I. INTRODUCTION

A technique based on genetic algorithms for the parameter estimation of the top oil temperature nonlinear model is discussed[1]. An investigation on a voltage regulator for parallel operated isolated asynchronous generators (IAGs) supplying three-phase four-wire loads driven by constant speed prime mover like diesel engine, bio-mass, gasoline, etc. The proposed voltage regulator is realized using a static compensator (STATCOM) for providing the reactive power compensation, harmonic elimination and load balancing [2]. During various loading conditions, the active and reactive power generated by the SEIG is not sufficient. Therefore, fluctuations occur in systems voltage and frequency. The STATCOM delivers the required power to the system, maintains the frequency and voltage to be constant and improves power quality in the system. The STATCOM also manages the active power of the system by storing the excess power in the BESS and supplying it when needed in the night time. Various types of loads such as Linear RL load, Non-Linear load, and Dynamic load are taken into account to evaluate the performance of the hybrid microgrid system is described [3]. The wind energy block consisting of a double fed induction generator (DFIG) is equipped with maximum power point tracking (MPPT) algorithm. The control of DFIG consists of two converters, namely rotor side converter (RSC) and load side converter (LSC) connected back to back at dc link. The MPPT operation requires speed control, which is realized using field oriented control through RSC. The rotor position required for vector control is estimated with model reference and adaptive system algorithm. Under all these conditions, currents flowing through stator windings of DFIG are balanced with low total harmonics distortion (THD) [4]. A cost-effective compensator to suppress harmonics and compensate the power factor of all-electric shipboard power systems (SPSs) is described [5]. This paper presents exploits the ruggedness and cost-effective IG as a viable alternative for an expensive permanent magnet synchronous generator, which is invariably used in standalone small wind turbines [6]. A modified amplitude adaptive notch filter (AANF)-based control algorithm for managing the generated power from different energy sources in an autonomous microgrid is discussed [7]. Self-excited induction generators (SEIGs) are increasingly being used in small-capacity isolated applications for harnessing both conventional and renewable energy resources. These SEIGs suffer from poor voltage regulation even when driven by constant speed prime movers or fixed head hydro turbines. The suitability of

these SEIGs to regulate the terminal voltage is a key factor in deciding its use in various applications [8]. The excitation capacitors and load combined with the d-q model of the machine, together with the saturation is used to predict the dynamic behavior of the SEIG is described [9]. The MLMS is a modified control of basic LMS that utilizes the past gradient information to reach improved adaptation performance instead of using its current value. This control has removed the drawback of LMS algorithms such as weight convergence dependence on the selection of the step size parameter. Moreover, it is observed that with inputs having high noise components, the MLMS algorithm performs better [10]. In recent years, single-phase frequency-locked loops (FLLs) are gaining more popularity as a signal processing and synchronization tool in a wide variety of engineering applications. In the power and energy area, a basic structure in designing the majority of available single-phase FLLs is the second-order generalized integrator-based FLL (SOGI-FLL), which is a nonlinear feedback control system [11]. This paper demonstrates a solar photovoltaic (PV)-battery energy storage (BES) based microgrid system with multifunctional voltage source converter (VSC) [12]. This article proposes an adaptive version of EPLL whose gain adjusts automatically with the variation of error. Adaptive EPLL (A-EPLL) is developed for positive sequence extraction of load current and its performance is tested for active filter operation. A PV system is also connected at the DC link of the shunt active power filter (SAPF) and the developed controller is tested under dynamic load changes [13]. It proves that 3P-EPLL is not able to accurately estimate the amplitude, phase angle, and frequency of the grid in such cases. In order to correctly estimate the grid synchronous information even under the non ideal grid conditions, an improved 3P-EPLL combined with the multiple delayed signal cancellation (DSC) filters is proposed [14].

This paper presents a microgrid (MG) system, which includes wind-battery and photovoltaic-array. A doubly fed induction generator (DFIG) is used as a wind power generator (WPG). Peak power from the wind turbine is extracted using tip speed ratio (TSR) algorithm. Reactive power is provided by the rotor side converter (RSC). An improved discrete second order sequence filter-frequency locked loop (DSOSF-FLL) control is used for grid side converter (GSC). It maintains the DC-link voltage as well as regulates the reactive power at the grid. The battery with a bi-directional converter is connected to the common DC-link of the GSC, which is used to store the wind power at light-load condition. A solar PV array is connected at the point of common coupling (PCC) [15].

In this article, the event-triggered control problem for linear systems with uncertainties is addressed. A model-based dynamic event-triggered transmission strategy is proposed for linear systems, and for systems that can be decomposed into interconnected subsystems, a distributed model-based dynamic event-triggered transmission strategy is also proposed with transmission delays and transmission protocols in the networks. The whole systems are modeled into a hybrid system framework by introducing storage variables. Using stability theorems of hybrid systems, explicit designs of the transmission strategies are presented and asymptotic stability is guaranteed [16]. To accomplish feasible large-scale integration of distributed energy resources (DER) into the existing grid system, microgrid implementation has proven to be the most effective. This article reviews the vital aspects of DER based microgrid and presents simulations to investigate the impacts of DER sources, electric vehicles (EV), and energy storage system (ESS) on practicable architectures' resilient operation. The focus is primarily on the concept and definition of microgrid, comparison of control strategies (primary, secondary, and tertiary strategies), energy management strategies; power quality (PQ) issues associated with DER based microgrid, and state-of-the-art entities such as ESS and EV's applications toward microgrid reliability. Following discussion on the different attributes of DER sources-based microgrid, simulations are performed to verify the results of the past works on the effects of solar, wind energy sources, ESS, and EVs on the microgrid frequency response. Additional simulations are conducted to assess the influences of DERs, ESS, EVs, and their operational strategies on the microgrid reliability aspects [17]. All-pass filter (APF) passes all frequency components of a signal without altering their amplitude, but changes their phase [18]. A large number of three-phase phase-locked loops (PLLs) have been developed [19]. In this work a wind based standalone DG system is developed and the results are analyzed under various operating conditions. The entire system is designed in MATALB/Simulink.

II. RESEARCH METHODOLOGY

The proposed wind based distributed generation system is developed in MATLAB/Simulink environment. The methodology is divide as follows:

2.1 System configuration

Fig. 1 represents wind driven self excited induction generator, voltage source inverter, filtering inductors and battery system based distributed generation system. The most important aspect of the system is the current controlled VSC with self-supporting dc-link voltage (v_{dc}). At the dc link, battery system is connected, which stores the surplus power as well as it supplies power during a deficit. The VSC is connected in shunt through interfacing inductors, which provides voltage regulation, harmonics elimination, and load balancing while feeding a nonlinear load. Moreover, by using the interfacing inductors, high-frequency ripples are eliminated from the VSC currents whereas the auxiliary components of this system are passive filters (R_f and c_f), which is used to remove high-frequency ripple from the PCC voltages. At the AC side, a 3.7-kW wind turbine driven SEIG is used.
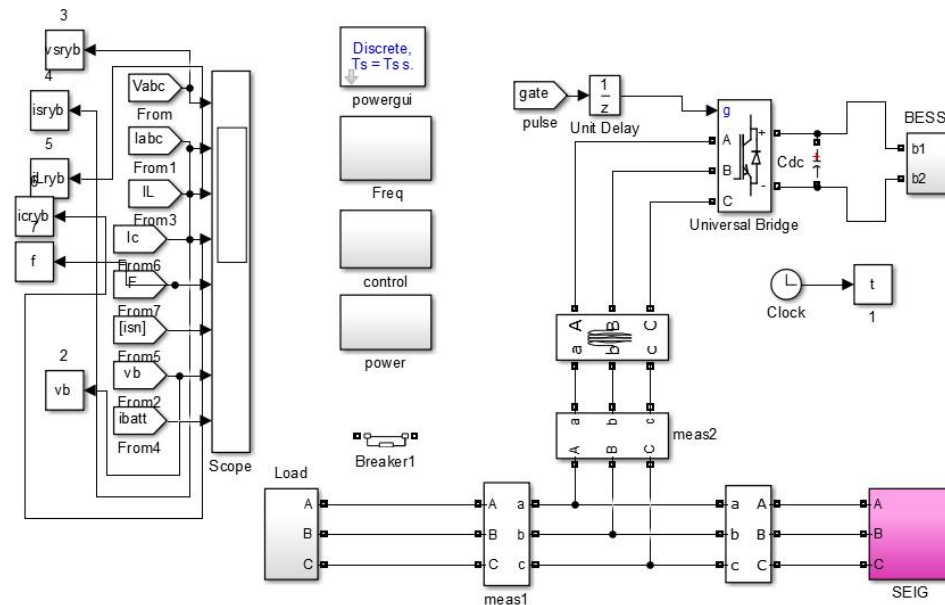
Fig. 1: Schematic diagram of wind based standalone system

Fig. 2 shows the design of wind turbine, capacitor bank and Simulink model of SEIG. The capacitor is utilized to provide reactive power to SEIG at no load. Further, a step input is used to vary the wind speed of wind turbine.
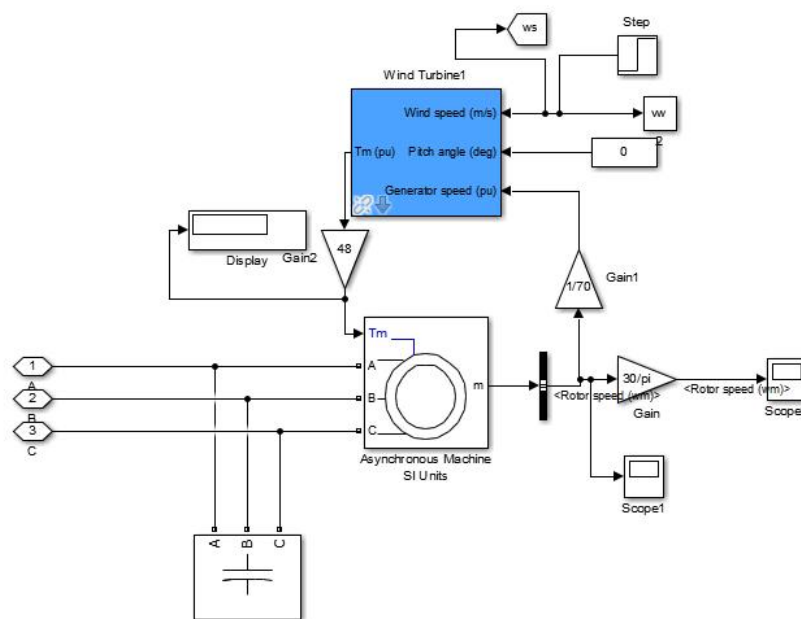
Fig. 2: SEIG and wind turbine

Fig. 3 represents a control scheme of distributed generation system. In this control scheme, a DSOGI-FLL based control is used to extract the fundamental current component under nonlinear load condition. Two PI controllers are also used to extract the active and quadrature current components. Further, extracted active and quadrature components are used to generate reference source current. The comparison of sensed current and reference source current is used to extract the triggering pulses for VSC.
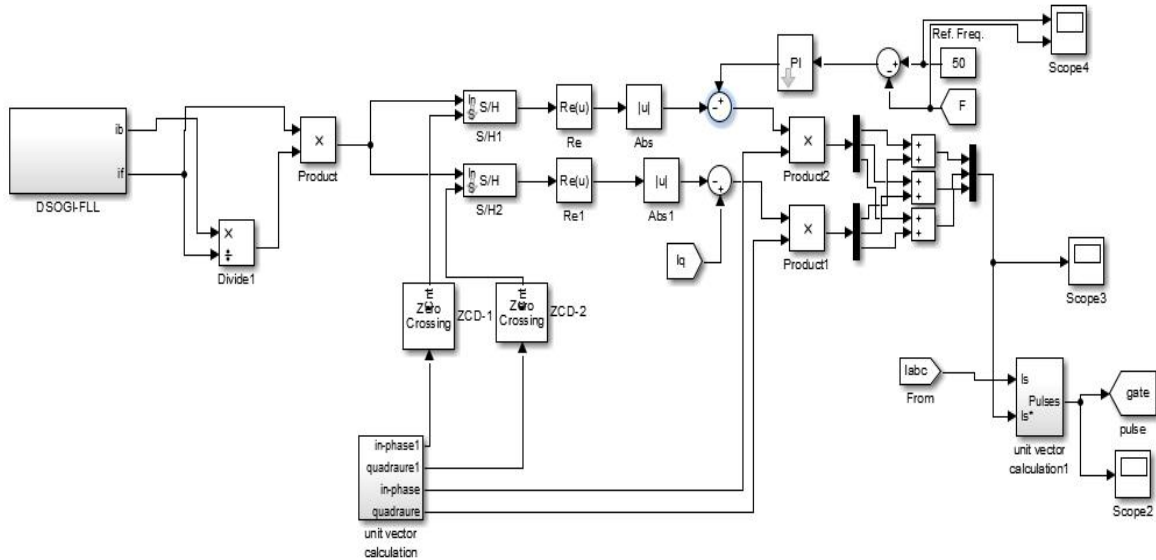

Fig. 3: Control Scheme

2.2 Calculation of phase angle, frequency and the amplitude of fundamental load current component

A DSOGI-FLL control algorithm is designed to evaluate the components such as phase angle, frequency and fundamental load current. Since the SOGI based FLL is a first order system, the tracking error cannot be eliminated completely. In the stationary reference frame, both α-axis and β-axis back EMFs are used for flux estimation. Considering that their frequencies are always identical, a single FLL combining the frequency error signals from both α-axis and β-axis could be used instead of two FLLs. In this case, the response might be improved, since double error information of the back EMF frequency is provided. Besides, the double-frequency component in the SOGI-based FLL might be eliminated in the DSOGI-based FLL, since the α-axis and the β-axis back EMFs are orthogonal. Therefore, the steady-state frequency error signal of DSOGI-based FLL is given by

$$\epsilon_f = \omega' x_a \epsilon_{ea} + \omega' x_\beta \epsilon_{e\beta} = \frac{x_\alpha^2 + x_\beta^2}{k}(\omega'^2 - \omega^2) \qquad (1)$$

$$\theta_1 = \tan^{-1}(i_{\beta1}/i_{\alpha1}) \qquad (2)$$

$$I_p = \sqrt{(i_{\alpha1})^2 + (i_{\beta1})^2} \qquad (3)$$

Amplitude of generator voltage and unit template generation

$$v_{ga} = \frac{1}{3}(2v_{ab} + v_{bc}) \qquad (4)$$

$$v_{gb} = \frac{1}{3}(-v_{ab} + v_{bc}) \qquad (5)$$

$$v_{gc} = \frac{1}{3}(-v_{ab} - 2v_{bc}) \qquad (6)$$

The quadrature and in-phase unit vector are extracted from the peak value of generator voltage and it is calculated as

$$V_t = \sqrt{\frac{2}{3}} \times \sqrt{v_{ga}^2 + v_{gb}^2 + v_{gc}^2} \qquad (7)$$

The in-phase unit vector are evaluated as

$$u_{pa} = \frac{v_{ga}}{V_t}, \; u_{pb} = \frac{v_{gb}}{V_t}, \text{ and } u_{pc} = \frac{v_{gc}}{V_t} \tag{8}$$

The quadrature unit vectors are evaluated by using the in-phase unit vectors and it is calculated as

$$u_{qa} = \frac{u_{pa}}{\sqrt{3}} + \frac{u_{pc}}{\sqrt{3}} \tag{9}$$

$$u_{qb} = \frac{\sqrt{3}u_{pa}}{2} + \frac{(u_{pb} - u_{pc})}{\sqrt{3}} \tag{10}$$

$$u_{qc} = \frac{\sqrt{3}u_{pa}}{2} + \frac{(u_{pb} - u_{pc})}{2\sqrt{3}} \tag{11}$$

2.3 Switching Pulses Generation for VSC

The DSOGI-FLL based control scheme for the generation of switching pulses for VSC is illustrated in Fig. 1. The load current input is given to the abc to αβ stationary frame. The DSOGI based FLL estimates the phase angle and peal value of fundamental load current. The peak value of the active/reactive component of the load current can be get by using two different sample and hold (S/H) circuits and zero crossing detectors (ZCD). The in-phase/quadrature unit vectors yields input to ZCD, the ZCD generates edge triggering pulses for S/H. The output of S/H is given to the low pass filter (LPF) and this produces active component of load current. Similarly, a parallel computation path is used for the evaluation of reactive component of load current.

The generator voltage is fed to the 3-phase PLL to determine the actual value of the frequency. The error between the actual frequency and reference frequency is fed to the DC voltage PI controller. The summation of the output of PI controller and PV current is subtracted from active load current component, which yields active component for reference generator current.

$$i_{Ld} = i_{pa} - i_{Lfa} \tag{12}$$

$$i_{Ld}^* = i_{Ld} \times u_{pabc} \tag{13}$$

The peal value of reactive component of reference generator current is calculated as

$$i_{Lq} = i_q - i_{Lfq} \tag{14}$$

$$i_{Lq}^* = i_{Lq} \times u_{qabc} \tag{15}$$

The summation of equation (14) and (15) yields the reference generator current

$$i_{gabc}^* = i_{Ld}^* + i_{Lq}^* \tag{16}$$

For the generation of the VSC switching signal, the sensed reference generator current and extracted sinusoidal reference generator current are fed to the hysteresis controller.

III. RESULTS AND DISCUSSION

The steady state and dynamic performance of the proposed system is analyzed under different operating conditions. The DSOGI-FLL control algorithm extracts the fundamental component under unbalanced nonlinear load condition. The source voltage (v_{gabc}), source current (i_{gabc}), load current (i_{Labc}), compensator current (i_{cabc}), frequency (f), battery voltage (v_b) and battery current (i_b) are discussed. The battery system provides power support during intermittent conditions of wind speed and unbalanced load.

3.1 Dynamic Response of Proposed System under Unbalanced Load

Fig. 4 represents the dynamic response of DG system under unbalanced load condition. The load of phase 'a' is removed at t=1.6s and the load of phase 'a' is connected at t=1.8s. The source current and compensator current are increased and load current is decreased during the load removal duration. The controller maintains the source voltage and frequency of the system. The proposed control with VSC provides voltage/frequency regulation, power support, harmonic elimination and improves the power quality of the standalone DG system.
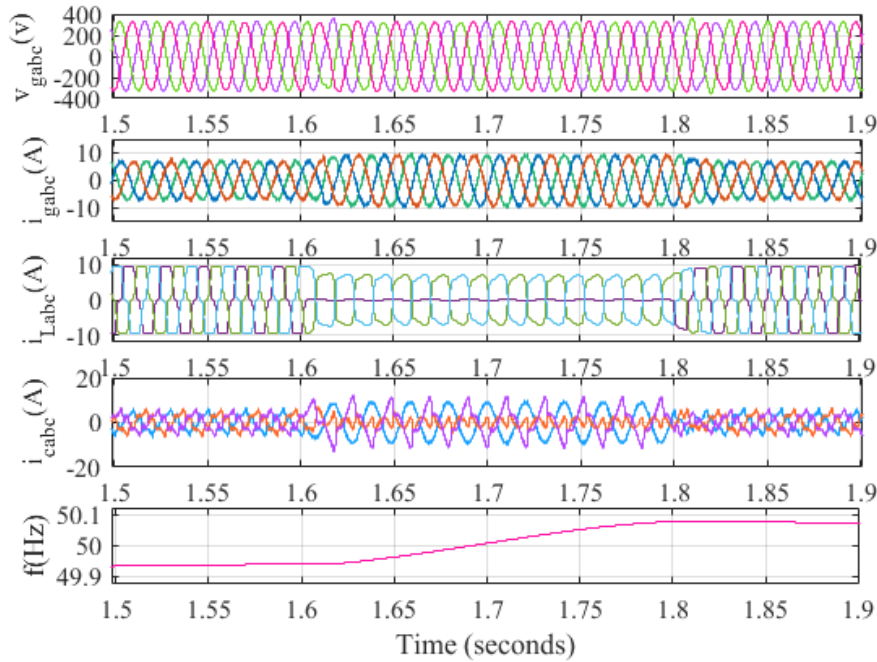
Fig. 4 Dynamic response of DG system under unbalanced load.

3.2 Dynamic Response of DG System under Varying Speed

Fig. 5 shows the dynamic response of DG system under varying speed and balanced nonlinear load. The wind speed is changed from 17 m/s to 13 m/s at t=1.7s. During the variation in wind speed, the compensator current is increased and delivered the required power at PCC during dynamic conditions of wind. The controller maintains constant the parameters such as voltage, frequency and source current during intermittent condition of wind.
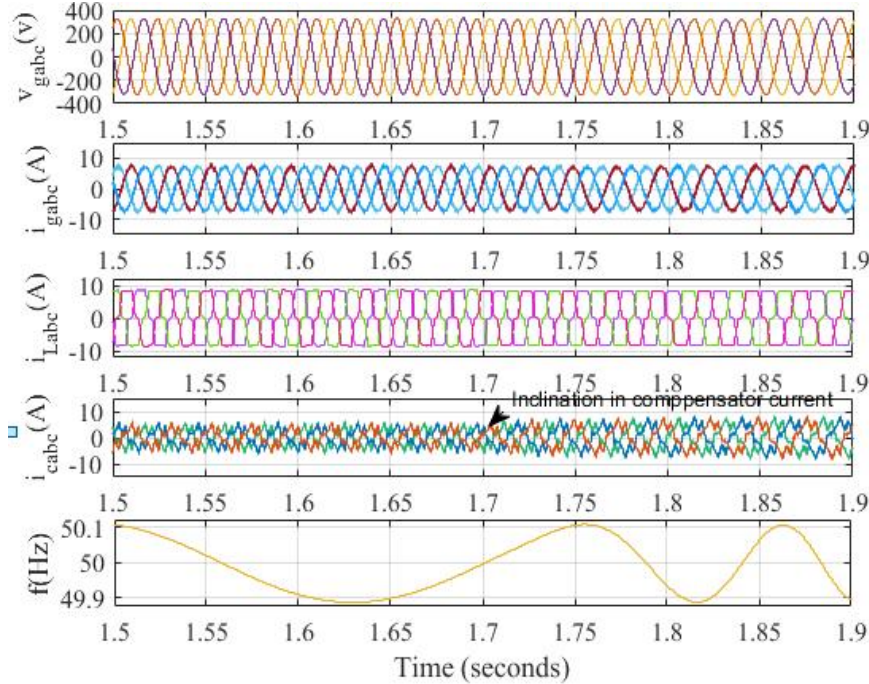

Fig. 5 Dynamic response of DG system under varying wind speed

3.3 Battery Response under Different Operating Conditions

Fig. 6(a) and (b) shows the dynamic response of battery system under unbalanced load and varying wind speed. Fig. 6(a) shows the dynamic response of battery system under unbalanced loading. The load is removed of phase 'a' at t=1.6s to t=1.8s of the DG system. During the removal of load battery current is increased and the extra power is supplied to the battery during removal of load. Fig. 6(b) shows the dynamic response of battery system at varying wind speed. The wind speed is reducing from 17 m/s to 13 m/s at t=1.s. The battery charging current is decreased during variation in wind. The battery is supplied the required power at point of common coupling.
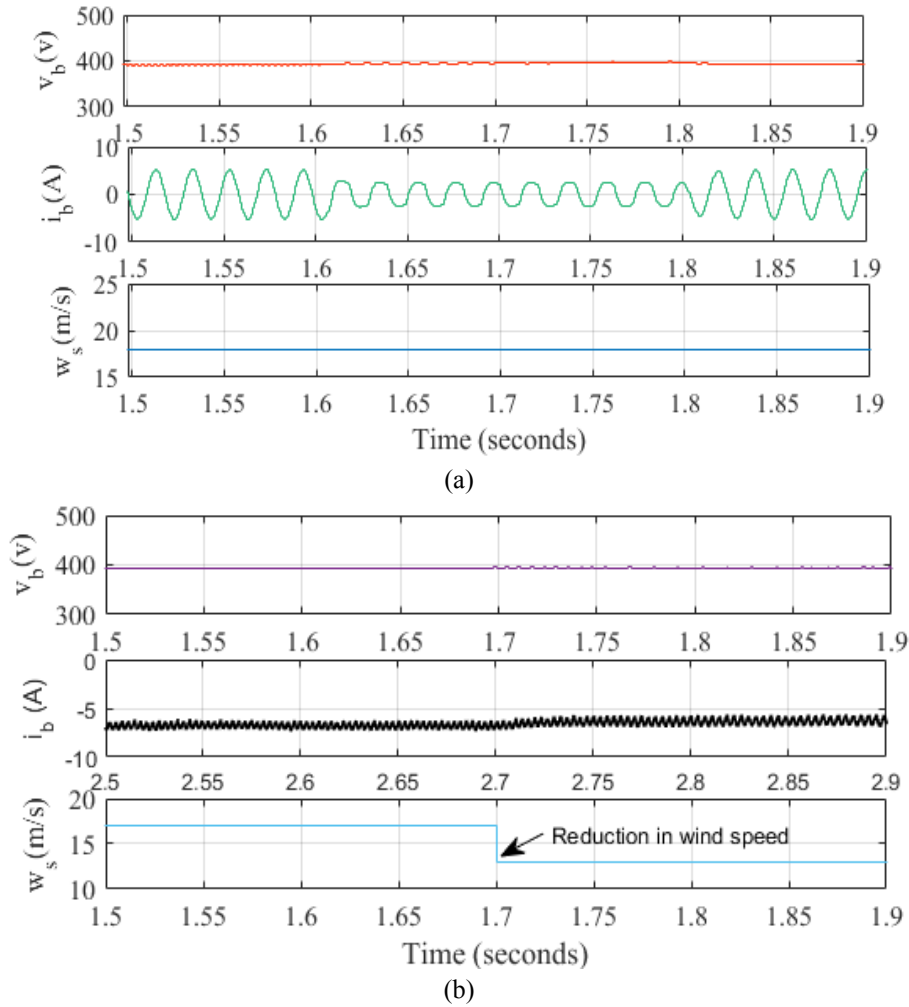

(a)

(b)

Fig. 6(a) and (b) Battery response under dynamic condition

3.4 Steady State Response of Proposed DG System

Fig. 7(a)-(c) represents the steady state response of standalone DG system under nonlinear load condition. The THD of source voltage, source current and load current are 3.15%, 4.88% and 27.74% respectively, which is according to the IEEE-519 standard.
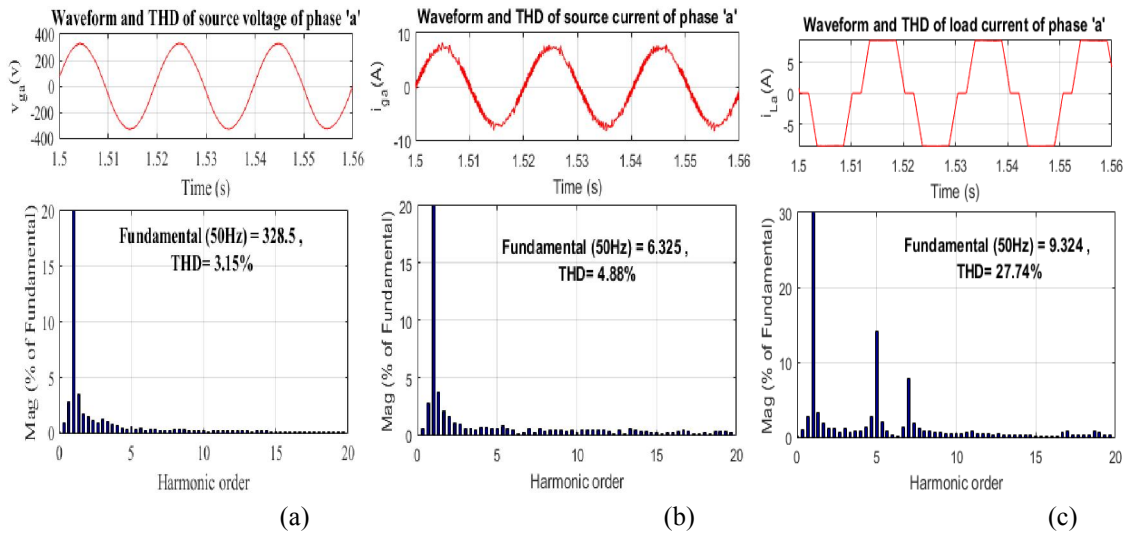
Fig. 7(a)-(c) Steady state analysis of Source voltage, source current and load current

IV. CONCLUSION AND FUTURE SCOPE

In this work, a DSOGI-FLL control algorithm has been used for distributed generation system for standalone applications. The steady state and dynamic performance of the proposed system is analyzed under different operating condition such as varying wind speed and unbalanced load. The DSOGI-FLL -based control has extracted the fundamental component of nonlinear load currents to maintain balanced and sinusoidal source current during worst condition of load. The battery system consumes the extra power and delivers the power at PCC during high load demand. Simulated results have illustrated that the control is effective in reactive power compensation, load balancing, harmonics elimination, and it has worked as a DSTATCOM. Moreover, Simulation results obtained for the system, especially source voltage and source current are in accordance with the IEEE-519 standard.

The proposed DG system are local energy grids the can disconnect from the traditional grid and operate autonomously. DG systems have the ability to strengthen and reinforce the traditional grid because they can function even when the main grid is down and are optimal for integrating renewable sources of energy. The proposed system with suitable controller can be used for electrical vehicle supply and supply to single phase loads.

REFERENCES

[1] S. Xie, X. Wang, C. Qu, X. Wang, and J. Guo, "Impacts of different wind speed simulation methods on conditional reliability indices," Int. Trans. Electr. energy Syst., vol. 20, no. June 2009, pp. 1–6, 2013, doi: 10.1002/etep.

[2] G. K. Kasal and B. Singh, "A STATCOM based voltage regulator for parallel operated isolated asynchronous generators feeding three-phase four-wire loads," Int. J. Power Electron., vol. 1, no. 3, pp. 318–332, 2009, doi: 10.1504/IJPElec.2009.023625.

[3] B. Jena and A. Choudhury, "Voltage and frequency stabilisation in a micro-hydro-PV based hybrid microgrid using FLC based STATCOM equipped with BESS," Proc. IEEE Int. Conf. Circuit, Power Comput. Technol. ICCPCT 2017, 2017, doi: 10.1109/ICCPCT.2017.8074291.

[4] N. K. S. Naidu and B. Singh, "Grid-Interfaced DFIG-Based Variable Speed Wind Energy Conversion System With Power Smoothening," IEEE Trans. Sustain. Energy, vol. 8, no. 1, pp. 51–58, 2017, doi: 10.1109/TSTE.2016.2582520.

[5] Y. Terriche et al., "A Hybrid Compensator Configuration for VAR Control and Harmonic Suppression in All-Electric Shipboard Power Systems," IEEE Trans. Power Deliv., vol. 35, no. 3, pp. 1379–1389, Jun. 2020, doi: 10.1109/TPWRD.2019.2943523.

[6] S. L. Prakash, M. Arutchelvi, and A. S. Jesudaiyan, "Autonomous PV-Array Excited Wind-Driven Induction Generator for Off-Grid Application in India," IEEE J. Emerg. Sel. Top. Power Electron., vol. 4, no. 4, pp. 1259–1269, 2016, doi: 10.1109/JESTPE.2016.2579678.

[7] S. Kewat and B. Singh, "Modified amplitude adaptive control algorithm for power quality improvement in multiple

distributed generation system," IET Power Electron., vol. 12, no. 9, pp. 2321–2329, Aug. 2019, doi: 10.1049/iet-pel.2018.5936.

[8] Y. K. Chauhan, S. K. Jain, and B. Singh, "A prospective on voltage regulation of self-excited induction genezators for industry applications," IEEE Trans. Ind. Appl., vol. 46, no. 2, pp. 720–730, 2010, doi: 10.1109/TIA.2009.2039984.

[9] S. S. Murthy and A. J. P. Pinto, "A generalized dynamic and steady state analysis of Self Excited Induction Generator (SEIG) based on MATLAB," ICEMS 2005 Proc. Eighth Int. Conf. Electr. Mach. Syst., vol. 3, pp. 1933–1938, 2005, doi: 10.1109/icems.2005.202898.

[10] A. K. Giri, S. R. Arya, and R. Maurya, "Compensation of Power Quality Problems in Wind-Based Renewable Energy System for Small Consumer as Isolated Loads," IEEE Trans. Ind. Electron., vol. 66, no. 11, pp. 9023–9031, Nov. 2019, doi: 10.1109/TIE.2018.2873515.

[11] S. Golestan, J. M. Guerrero, J. C. Vasquez, A. M. Abusorrah, and Y. Al-Turki, "Standard SOGI-FLL and Its Close Variants: Precise Modeling in LTP Framework and Determining Stability Region/Robustness Metrics," IEEE Trans. Power Electron., vol. 36, no. 1, pp. 409–422, 2021, doi: 10.1109/TPEL.2020.2997603.

[12] V. Narayanan, Seema, and B. Singh, "Solar PV-BES based microgrid system with seamless transition capability," 2018 2nd IEEE Int. Conf. Power Electron. Intell. Control Energy Syst. ICPEICES 2018, pp. 722–728, 2018, doi: 10.1109/ICPEICES.2018.8897358.

[13] P. Chittora, A. Singh, and M. Singh, "Adaptive EPLL for improving power quality in three-phase three-wire grid-connected photovoltaic system," IET Renewable Power Generation, vol. 13, no. 9. pp. 1595–1602, 2019, doi: 10.1049/iet-rpg.2018.5261.

[14] F. Wu and X. Li, "Multiple DSC Filter-Based Three-Phase EPLL for Nonideal Grid Synchronization," IEEE J. Emerg. Sel. Top. Power Electron., vol. 5, no. 3, pp. 1396–1403, 2017, doi: 10.1109/JESTPE.2017.2701498.

[15] S. Bhattacharyya and B. Singh, "Wind-Battery-PV Based Microgrid with Discrete Second Order Sequence Filter-Frequency Locked Loop," Proc. 2020 IEEE Int. Conf. Power, Instrumentation, Control Comput. PICC 2020, 2020, doi: 10.1109/PICC51425.2020.9362357.

[16] K. Z. Liu, A. R. Teel, X. M. Sun, and X. F. Wang, "Model-Based Dynamic Event-Triggered Control for Systems with Uncertainty: A Hybrid System Approach," IEEE Trans. Automat. Contr., vol. 66, no. 1, pp. 444–451, 2021, doi: 10.1109/TAC.2020.2979788.

[17] A. Muhtadi, D. Pandit, N. Nguyen, and J. Mitra, "Distributed Energy Resources Based Microgrid: Review of Architecture, Control, and Reliability," IEEE Trans. Ind. Appl., vol. 57, no. 3, pp. 2223–2235, 2021, doi: 10.1109/TIA.2021.3065329.

[18] S. Golestan, J. M. Guerrero, J. C. Vasquez, A. M. Abusorrah, and Y. Al-Turki, "All-Pass-Filter-Based PLL Systems: Linear Modeling, Analysis, and Comparative Evaluation," IEEE Trans. Power Electron., vol. 35, no. 4, pp. 3558–3572, 2020, doi: 10.1109/TPEL.2019.2937936.

[19] M. Ramezani, S. Golestan, S. Li, and J. M. Guerrero, "A Simple Approach to Enhance the Performance of Complex-Coefficient Filter-Based PLL in Grid-Connected Applications," IEEE Trans. Ind. Electron., vol. 65, no. 6, pp. 5081–5085, 2018, doi: 10.1109/TIE.2017.2772164.